Applied Acoustics 83 (2014) 123–126

Contents lists available at ScienceDirect

Applied Acoustics

journal homepage: www.elsevier.com/locate/apacoust

Temperature and frequency dependence of the visco-elasticity of a poro-elastic layer

C. Glorieux [a,*], J. Descheemaeker [a], Jan Vandenbroeck [b], J.-P. Groby [c], L. Boeckx [d], P. Khurana [a], N.B. Roozen [a]

[a] KU Leuven, Celestijnenlaan 200D, 3001 Heverlee, Belgium
[b] Computational Physics & Foam Technology, Core Science Group, Huntsman Polyurethanes, Everslaan 45, B3078 Everberg, Belgium
[c] LAUM UMR CNRS 6613, Université du Maine, Avenue Olivier Messiaen, 72085 Le Mans, France
[d] VK Engineering, Axxes Business Park, Guldensporenpark Building A No 4, 9820 Merelbeke, Belgium

ARTICLE INFO

Article history:
Received 14 September 2013
Received in revised form 4 March 2014
Accepted 12 March 2014
Available online 20 April 2014

Keywords:
Porous material
Characterization
Temperature effects

ABSTRACT

Besides their structural complexity, the acoustic behavior of polymer-based poro-elastic layers is complicated also due to their frequency dependent elasticity. In this work, we address the frequency and temperature dependence of the elastic behavior in general, and the shear modulus in particular, of poro-visco-elastic materials. The analysis is based on the monitoring of mechanically excited guided acoustic wave propagation by means of a laser Doppler vibrometer scanning technique. The concept and practical implementation of the experimental method are presented, as well as the signal processing procedure and data analysis. Experimental data are presented for a polyurethane foam. The observed visco-elastic behavior, complemented with dielectric spectroscopy data, is interpreted in the framework of two underlying relaxation processes.

1. Introduction

The elasticity of porous materials plays a key role in their acoustic and mechanical behavior, which are crucial for many applications, such as acoustic absorption and vibration damping. Even in the linear regime of elasticity, the relation between the bulk elasticity of the polymer of which the frame of cellular materials consists, and the effective, macroscopic frame elasticity is quite complicated. With respect to the macroscopic shear modulus, for not too high frequencies, the situation gets simplified, since the (non-viscous) fluid filling the pores does not have to be taken into account in the analysis. Quite some work has been performed on the development of theoretical models connecting the elastic moduli of the frame material in bulk form, the microscopic cell wall dimensions and the microscopic morphology on one hand, to the macroscopic elasticity on the other hand [1]. In a model proposed by Gibson and Ashby [2], the relation between the macroscopic frame's Young's (E) and shear (G) modulus on one hand, and the Young's modulus of the bulk material (E_s) on the other hand, is given by:

$$E, G \sim E_s \left(\frac{\rho}{\rho_s}\right)^2, \tag{1}$$

where the ratio between the volume density of the bulk material, ρ_s, and the frame density, ρ, make an important part of the proportionality, expressing that the material softens with increasing porosity.

An additional challenge that is encountered in this matter is how to predict the macroscopic frame damping. Indeed, besides the contribution to the acoustic wave attenuation for the airborne wave of the porous morphology (imaginary parts of Biot parameters [3] and attenuation due to scattering), which is mainly important towards higher frequencies, also the contribution due to non-zero imaginary parts of the elastic moduli of the frame is of high importance for the global attenuation behavior. The latter contribution relates to the visco-elastic nature of many frame materials, in particular for polymer foams. Besides the technological interest to understand and predict the effective acoustic attenuation and effective elastic damping by the frame, starting from the visco-elastic behavior of the bulk frame material and from the geometrical frame parameters, the relation between the bulk behavior and porous behavior is also quite intriguing from the physics point of view. The phenomenology of the glass transition in bulk visco-elastic materials is better and better understood, but much less

* Corresponding author.
E-mail address: christ.glorieux@fys.kuleuven.be (C. Glorieux).

http://dx.doi.org/10.1016/j.apacoust.2014.03.010
0003-682X/

research has been done on the link between the bulk level and the porous level. One could expect that the imaginary parts of the elastic moduli follow the same trend as Eq. (1), but with some mixing between the different moduli, due to the mixed motion on the microscopic level.

In the following, we contribute to clarifying the behavior by reporting on results for the temperature (245–301 K) and frequency (1200–4400 Hz) dependence of the shear modulus of a Urecom® (trademark of Recticel) poro-elastic layer of 5 cm thickness.

2. Determination of the shear modulus of a poro-elastic frame by guided wave propagation analysis

For the elastic characterization of the materials under study, we have made use of guided acoustic waves, whose propagation characteristics are closely connected with the material parameters via known theoretical models [4]. In principle the acoustic waves guided in our slabs of finite thickness are of the Lamb type. However, in the accessible frequency range between 1.2 and 4.4 kHz, the longitudinal and shear acoustic wavelengths, and thus the penetration depth of the guided waves, are significantly shorter (less than 3 cm) than the layer thickness of 5 cm, so that the waves are of the Rayleigh type, confined at the excitation side. Since Rayleigh waves are not subject to geometry-related dispersion, any measured dispersion or damping can be considered to be resulting from the intrinsic dispersion of the material. This feature makes Rayleigh waves more suitable than Lamb waves to study viscoelastic material dispersion and damping, in spite of the disadvantage that, contrary to Lamb wave dispersion analysis, they do not allow to simultaneously determine the two moduli (longitudinal/shear).

In earlier work we have shown that in the frequency range 1.2–4.4 kHz) the propagation of guided acoustic waves, excited and detected via the frame, is dominated by the frame properties, with negligible influence of the Biot parameters or of the fluid [5]. It turns out that for surface waves of the Rayleigh type, the wave propagation velocity is mainly determined by the shear modulus, and to a good approximation it can be considered independent of the longitudinal modulus. The shear modulus is proportional with the square of the shear wave velocity, with whom the Rayleigh velocity is roughly proportional.

In our experimental setup quasi-monochromatic Rayleigh wave burst packets were generated by means of a shaker. Their velocity and damping were determined by analyzing the time of arrival Δt and (average burst) amplitude A of free-running wave signals, measured by means of laser-Doppler vibrometry, at different distances Δx from the source, over a range between 5 and 30 cm, depending on the damping distance. The quality of the signal was enhanced by placing (acoustically thin) retro-reflective stickers along the path of interest. The time of arrival of a wave signal was determined by cross-correlating it with the burst of 5–20 cycles. The burst signal was generated by an Agilent 33120A function generator which was amplified by a Bruel and Kjaer type 2706 amplifier and send to an LMS Qsources shaker. The velocity of the waves was then determined from the slope of the linear curve of Δx versus Δt. The damping was determined by fitting an exponential decay function to A(x). The analysis was done in the temperature range between 245 and 301 K and for frequency between 1200 Hz and 4400 Hz. As a result of the increasing wavelength with decreasing frequency, the burst length below 1 kHz became too long with respect to the maximum distance range between the generation and detection site. Above 4.4 kHz, due to increased damping, the signal-to-noise ratio was too weak for adequate analysis.

Table 1
Material properties of the investigated Urecom® material.

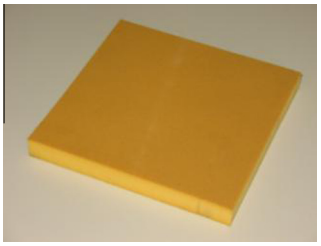

Porosity ϕ	$\geqslant 0.95$
Density ρ	(96 ± 4) kg m^{-3}
Tortuosity	1.5 ± 0.1
Flow resistivity σ	(400 ± 3) kN s m^{-4}
Viscous characteristic length Λ	(60 ± 7) μm
Thermal characteristic length Λ'	(119 ± 12) μm

The temperature of the sample was controlled by placing it in a temperature controlled atmosphere, in which the sample surface was optically accessible for the vibrometer via a window.

The material properties of the investigated Urecom® (trademark from Recticel) material are listed in Table 1.

3. Temperature and frequency dependence of the phase velocity of the real and imaginary part of the Rayleigh wave propagation velocity

Fig. 1 shows the experimental results for the frequency dependence of the phase velocity (a) and the attenuation coefficient (b) of the Rayleigh wave along the 5 cm acoustically thick Urecom® sample under investigation at different temperatures. The phase velocity c (m/s) and the attenuation coefficient α (Np/m) are calculated from the measured (complex) wavenumber k as follows (e.g. see [6]):

$$c = \mathrm{Re}\{\frac{\omega}{k}\} \quad \alpha = \mathrm{Im}\{k\} \tag{2}$$

where c is the phase constant in radians per metre (rad/m) and α is the attenuation constant in Nepers per metre (Np/m).

Fig. 2 depicts the same data, but in the form of the temperature dependence at different frequencies. Given that Poisson's ratio for this kind of material typically only varies between 0.20 and 0.25, the Rayleigh velocity is roughly proportional with the shear

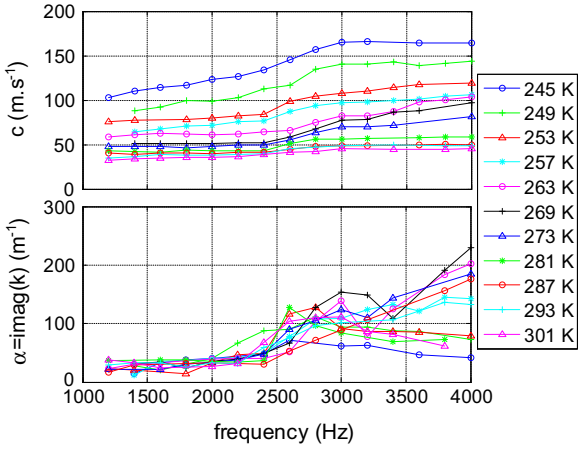

Fig. 1. Frequency dependence of the real part of the propagation velocity (top) and the imaginary part of the wavenumber (bottom) of Rayleigh waves in Urecom® polyurethane as function of frequency, for different temperatures.

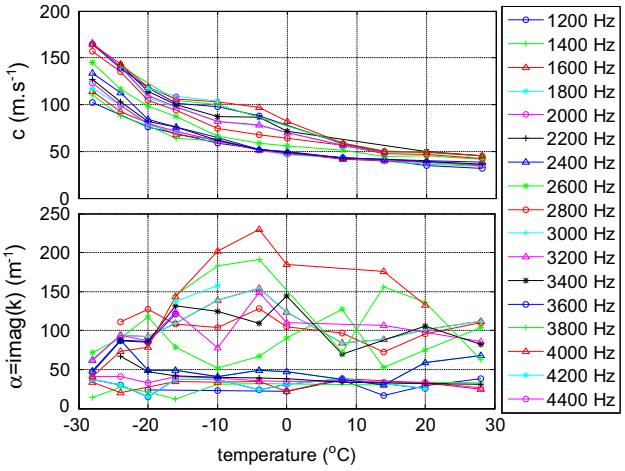

Fig. 2. Frequency dependence of the real part of the propagation velocity (top) and the imaginary part of the wavenumber (bottom) of Rayleigh waves in Urecom® polyurethane as function of temperature, for different frequencies.

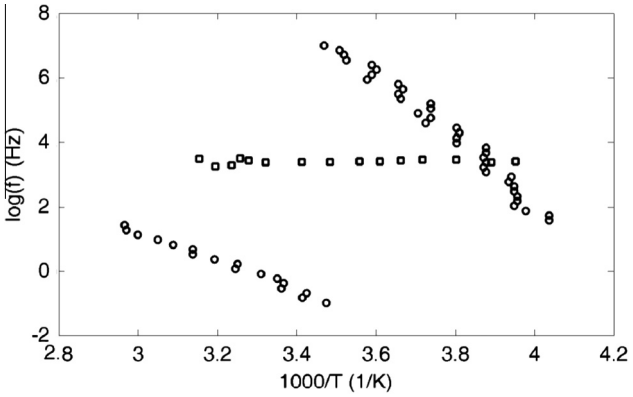

Fig. 3. Arrhenius plot of the relaxation frequencies of two rotational processes (circles in SW and NE part of the figure) as determined by dielectric spectroscopy, together with the frequency (squares) of the inflection point of the $c(f)$ Rayleigh velocity curve for Urecom® polyurethane.

velocity, which in turn is proportional with the square root of the shear modulus, so that the experimental data are also qualitatively representative for the behavior of the shear modulus with temperature and frequency.

To some extent, the phase velocity c behaves as expected. The shear velocity, which is representative for the material's shear stiffness, increases with increasing frequency, while the material softens with increasing temperature. For a simple visco-elastic material, one would expect S-curve like behavior with temperature and with frequency, with a shifting declination point with changing frequency respectively temperature. For typical visco-elastic materials, the asymptotic limits of all shifted S-curves are coincident, and the shift of the relaxation frequency (corresponding with the declination point of $c(f)$) with temperature is very rapid.

The $c(f)$ curves in Fig. 2 appear to have S-type behavior, however, the increase of the relaxation frequency with increasing temperature is very small compared to classical Arrhenius or VFT behavior [7]. Moreover, unlike classical visco-elastic materials, the low- and high-temperature limit of the curves are not coincident. The latter observation could be ascribed to the small width of the experimentally accessible frequency range, but the first one requires a closer look. Due to the Kramers–Kronig relation, the declination points of $c(f)$ curves should go along with a maximum in the damping curves, here represented by the imaginary part of the wave number. Fig. 1 does not show clear maxima, though the experimental uncertainty prevents to exclude the possibility that weak damping peaks would be superposed on a rising background.

In order to get a grasp on the observed behavior, we have also performed dielectric spectroscopy measurements, which allow to map the orientational relaxation behavior in a very wide temperature and frequency range. Two orientational processes were found. The temperature dependence of the respective relaxation frequencies are shown, together with the frequencies extracted from the declination points of the acoustic data, in the Arrhenius plot in Fig. 3. From this comparison, it is obvious that the characteristic acoustic frequencies cannot be interpreted as relaxation frequencies: their temperature dependence is totally different from the relaxation frequencies of the 2 rotational processes. On the other hand, the occurrence of two rotational relaxation processes with very different temperature behavior, together with the typical hard/soft copolymer–segment–structure of polyurethane elastomers, infers that the mechanical/acoustical behavior is the result of two very different types of microscopic elastic responses so that single Debye behavior should not be expected, neither should it be possible to perform temperature-frequency superposition and rescale all data to one master curve .

One can expect that it would be possible to fit the temperature and frequency dependence of the complex shear modulus, $G(\omega,T)$, extracted from the data by a combination of two Debye processes, or, more probable, Havriliak–Negami, functions with VFT dependence of the respective relaxation frequencies, as follows:

$$G(\omega,T) = G_0 + \frac{\Delta G_1}{\left(1+i\left(\frac{\omega}{\omega_1(T)}\right)^{\alpha_1}\right)^{\beta_1}} + \frac{\Delta G_1}{\left(1+i\left(\frac{\omega}{\omega_2(T)}\right)^{\alpha_2}\right)^{\beta_2}}, \tag{3}$$

with α_j and β_j the Havriliak–Negami parameters of the processes (j = 1,2), $\omega_j(T)$ the angular relaxation frequencies, G_0 the steady state shear modulus, and ΔG_j the relaxation strengths. $\omega_{j,\infty}$ are the high temperature limits of the angular relaxation frequencies, B_j and T_{0j} are the parameters in the VFT relations:

$$\omega_j(T) = \omega_{j,\infty} \exp\left(-\frac{B_j}{T-T_{0j}}\right). \tag{4}$$

The knowledge of $\omega_{1,\mathrm{rotation}}(T)$ and $\omega_{2,\mathrm{rotation}}(T)$ from the dielectric experiment could help to estimate their mechanical equivalents $\omega_1(T)$ and $\omega_2(T)$, which are expected to be different from the rotational angular frequencies only by a temperature independent factor. However, given the large remaining number of unknown parameters, and the narrow accessible frequency range, it is in practice not straightforward to perform a reliable fit. Due to very high damping, it is unlikely that alternative techniques would allow to get reliable data above 4000 Hz. One possible scheme could be to excite the sample with a comb-like transducer with spatially periodic grating structure, and optically detect the periodical wave package within the excitation region, as it is successfully done in the impulsive stimulated scattering technique that makes use of a laser-induced transient thermal grating [8].

Efforts are ongoing to extend the data to lower frequencies, by making use of Dynamical Mechanical Thermal Analysis (DMTA) for frequencies below 100 Hz down to 10 mHz, and resonant methods spanning the range between 100 and 1200 Hz. Together with those methods, the here proposed guided wave technique thus has the potential to access almost 6 orders of magnitude in frequency, which should be sufficient to reliably resolve the two distributions of relaxation distributions underlying the global visco-elastic behavior, and to unravel the two underlying types of microscopic elastic responses.

Acknowledgement

The authors would like to thank the KU Leuven Research Council (project OT/11/064) and the European Commission (Marie Curie Grant, FP7-PEOPLE-2011-IEF, Grant Agreement Number PIEF-GA-2011-298278, Project acronym PAM, Project title "the Physics of Acoustic Materials") for financial support.

References

[1] Hilyard NC, Cunningham A. Low density cellular plastics. Cambridge, UK: Chapman & Hall, University Press; 1994, ISBN 0 412 58410 7.
[2] Gibson LJ, Ashby MF. Cellular solids. Cambridge University Press; 1997, ISBN 0 521 49911 9.
[3] Allard JF, Atalla N. Propagation of sound in porous media – modeling sound absorbing materials. Chichester: Wiley; 2009, ISBN 978 0470746615.
[4] Viktorov IA. Rayleigh and lamb waves: physical theory and applications. New York, USA: Plenum Press; 1967, ISBN 0306302861.
[5] Descheemaeker J, Glorieux C, Lauriks W, Groby JP, Leclaire P, Boeckx L. Acta Acustica United Acustica 2011;97:734–43.
[6] Boeckx L, Leclaire P, Khurana P, Glorieux C, Lauriks W, Allard JF. Guided elastic waves in porous materials saturated by air under Lamb conditions. J Appl Phys 2005;97.
[7] Donth E. The glass transition: relaxation dynamics in liquids and disordered materials. Berlin: Springer Series in Materials Science (Springer-Verlag); 2001, ISBN 978-3-540-41801-6.
[8] Yan Y-X, Nelson KA. J Chem Phys 1987;87:6240–56.